

An approach to design a high power piezoelectric ultrasonic transducer

Amir Abdullah · Mohsen Shahini · Abbas Pak

Received: 25 December 2006 / Accepted: 18 December 2007 / Published online: 17 January 2008
© Springer Science + Business Media, LLC 2007

Abstract Application of ultrasonic waves has been considerably progressed during the last decade and piezoelectric ceramics have had a common use as the driving source of such waves. However, there is not enough documented information on design and technology of manufacturing a high power ultrasonic transducer. In this paper, an attempt has been made to analyze the stress produced along the oscillating PZT employed ultrasonic head by applying the principles of acoustic wave propagation. Then, based on such analysis, general principles of PZT transducer design, excited by a DC-biased alternating electrical source, has been derived and finally a typical such transducer has been designed, manufactured and tested. By employing finite element modal analysis, the resonance frequency of the transducer was determined and compared with the experimental results. It was concluded that, the constitutive piezoelectric equations referred to in most sources and books are not valid for analyzing the acoustical dynamic stress in ultrasonic transducers. Instead, the analysis should be done with considering the dynamic behavior (elastic, damping and Inertia factors) of the problem.

Keywords Ultrasonic transducer · Piezoelectric · Acoustic · FEM analysis

1 Introduction

Since Prof. Langevin developed the first sandwich ultrasonic transducer by embedding piezoelectric rings between two metals and employed it for high intensity vibration, there have been great efforts in modeling and formulating such transducers. Of all proposed methods, Mason's has been found the best in design and analysis of PZT transducers. He has offered the Equivalent Circuit Method (ECM) [1, 2]. Finite Element Method (FEM) is also the most reliable one for analyzing the ultrasonic transducers [3, 4]. When studying thick high power ultrasonic radiators, Mori et al. [5, 6] innovated a new method called Apparent Elasticity Method. Using this method, in investigating resonant frequency of sandwich transducers, it was observed that, as expected, resonant frequency is affected not only by physical and mechanical characteristic of elements and axial dimensions, but also by lateral dimensions and cross section of the transducer [7]. Hirase et al. [8] have explained variation of high-power PZT transducer parameters and mechanical losses, in particular, in resonant and anti-resonant frequencies and they have consequently recommended tuning in anti-resonant frequency for higher quality factor. According to Powell and Hayward's [9] findings at a Center for Ultrasonic Engineering in Strathclyde University in Scotland, acoustic power of transducer will increase by keeping the axial length constant and adding to the number of PZT rings used in the structure. However, coupling too many PZT layers requires further consideration unless piezo-composites and piezo-polymers are used, which have

A. Abdullah (✉)
Faculty of Mechanical Engineering,
Amirkabir University of Technology,
424 Hafez Ave.,
Tehran, Iran
e-mail: amirah@aut.ac.ir

M. Shahini
Mechanical Engineering Department, Toronto University,
Toronto, ON, Canada

A. Pak
School of Engineering, Tarbiat Modarres University,
Tehran, Iran

much lower quality factor and accordingly are less sensitive to the external load. The present study deals with the general principles of the design of PZT transducers that are excited by a DC biased alternating electrical source.

2 Assumptions

For simplifications, the following assumptions have been made:

Lateral pressure on the transducer is zero and sinusoidal longitudinal plane waves propagate axially. Diameter variation along transducer is also far enough from the critical value. Meanwhile, the influence of fillets and chamfers in the corners are ignored. Therefore, lateral or radial modes of vibration are negligible and the problem is one-dimensional.

Maximum diameter of the transducer is less than a quarter of the sound wavelength and the relationship $c = \sqrt{Y/\rho}$ can be used with relatively accurate approximation (where c is the sound speed in media with elasticity module of Y and density of ρ) [10]. The total length of the transducer is appropriate to standing waves generation. Acoustic impedance of air is considered zero so that a transducer operating in air is said to be unloaded. An overall configuration of a sandwich piezoelectric transducer is illustrated in Fig. 1.

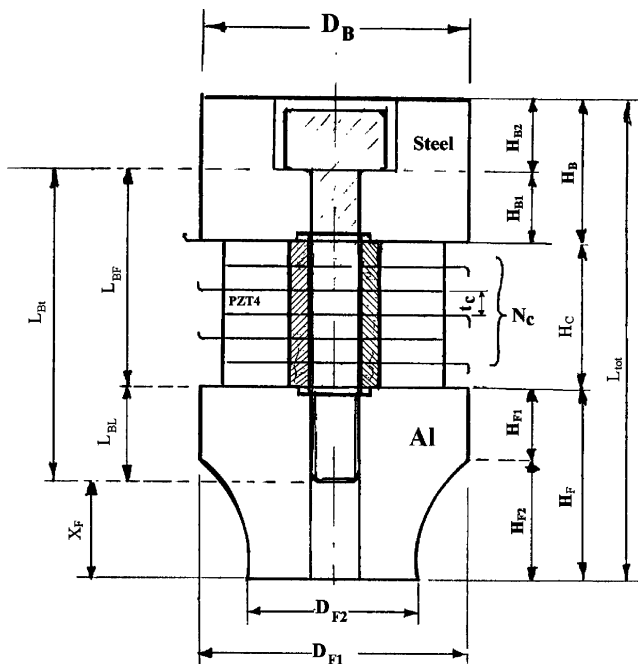


Fig. 1 Diagram of an ultrasonic transducer with its dimensions

3 Mathematical relations in piezoelectrics

Electromechanical equations of piezoelectric materials are as follows [10]:

$$S = TS^E + Ed \tag{1}$$

$$D = Td + \epsilon^T E \tag{2}$$

Where S is mechanical strain; T is stress (N/m^2); E is the applied electrical field (V/m); D is the displaced charge density (C/m^2); S^E , d and ϵ^T are physical characteristics of piezoelectrics namely compliance at constant electrical field (m^2/N), piezoelectric charge constant (m/V), and dielectric absolute permittivity under constant stress (F/m), respectively. If no stress on the piezo-electrics is applied:

$$S = dE = d \frac{V}{L} \tag{3}$$

Since $S = \frac{\Delta L}{L}$, then:

$$\Delta L = dV \tag{4}$$

4 Acoustic wave propagation equation in transducer

Displacement equation of a particle located at a point along a constant cross section bar material which is at distance x from the origin of harmonic source at the time t is:

$$\frac{\partial^2 \mu}{\partial t^2} = c^2 \frac{\partial^2 \mu}{\partial x^2} \tag{5}$$

Where μ is the displacement from the equilibrium. The strain developed from the unidimensional propagation of waves through the medium is obtained by:

$$S = \frac{\partial \mu}{\partial x} \tag{6}$$

Average acoustic wave intensity (W/m^2) is calculated to be [11]:

$$I = \frac{1}{2} \rho c \omega^2 \mu_0^2 = \frac{1}{2} T_{c \max}^2 / \rho c \tag{7}$$

ω is angular frequency of vibration in Hz ($=2\pi f$), μ_0 and $T_{c \max}$ are end point oscillation amplitude and nodal oscillatory stress amplitude respectively. Average acoustic power (W) is then derived as:

$$P = \frac{1}{2Y} T_{c \max}^2 cA \tag{8}$$

Where A (m^2) is cross sectional area and Y (N/m^2) is the Yung's modulus. It is obvious that $T_{c \max}$ must not cause

exceed over fatigue stress limit (T_f) of materials (piezoelectric and bolt) in the nodal plane (Fig. 2(b)). i.e.:

$$(T_{\max})_c \leq \frac{T_{fc}}{\beta} \text{ and } (T_{\max})_b = \frac{A_c T_{oc}}{A_b} + 2T_{b\max} \leq \frac{T_{fb}}{\gamma} \quad (9)$$

Where $(T_{\max})_c$ and $(T_{\max})_b$ are maximum tensile stress in ceramic material and bolt, respectively (see Fig. 2(b)), T_{oc} is the pre-stress pressure on the piezo-electrics, $T_{b\max}$ is the maximum amplitude of the dynamic stress in the bolt, T_{fc} and T_{fb} are fatigue stress limits for ceramic material and bolt, respectively, β and γ are the safety factors and A_c and A_b are ceramic and bolt cross sectional areas respectively. In resonance, displacement of any section normal to the

transducer axis along a cylindrical transducer with the length of $\lambda/2$ is expressed by:

$$\mu = \mu_0 \sin kx \sin \omega t \quad (10)$$

Where x is the distance from the vibration node of the transducer and $k = \omega/c$ is called the Wave Number. Hook's law and Eq. 6 lead to (Fig. 3):

$$T = Y \frac{\partial \mu}{\partial x} = Y \mu_0 k \cos kx \sin \omega t \quad (11)$$

As shown in Fig. 3 two ends of a half-wavelength transducer are the displacement antinodes, and there is a

Fig. 2 (a) and (b) Dynamic stress at nodal plane [(a) without prestress and excited with zero biased alternating voltage, (b) with prestress and excited with a DC-biased alternating voltage] (c) Length variation for prestressed piezoelectric and bolt under DC biased alternating voltage excitation

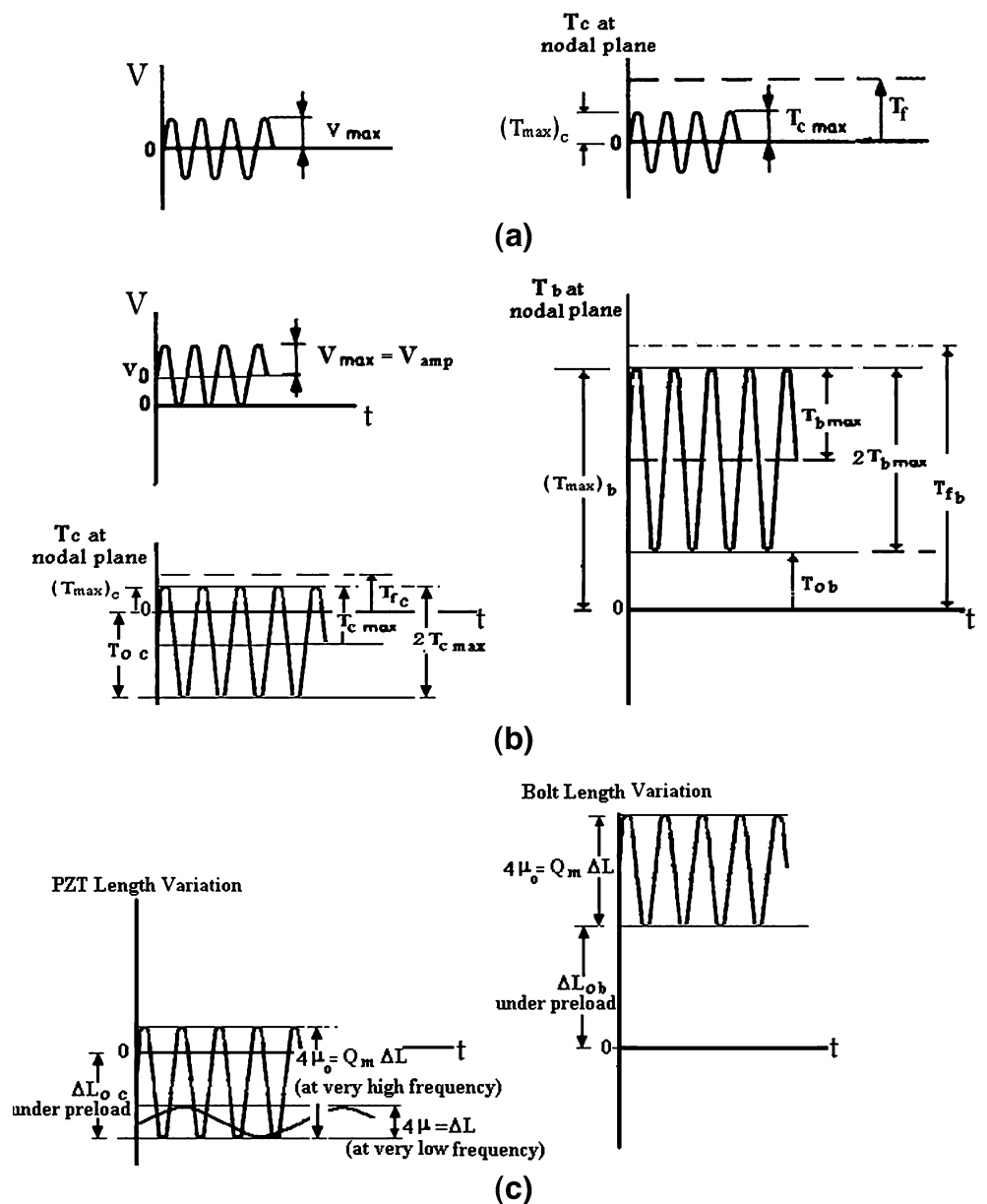
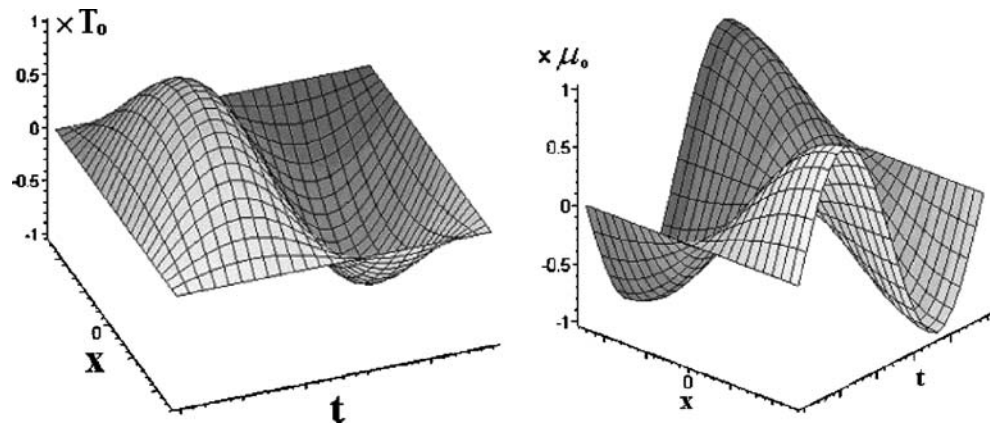


Fig. 3 Displacement (*right*) and stress (*left*) versus time along a transducer with the length of $\lambda/2$ and in resonance



displacement node at the middle of transducer, where the maximum oscillating stress amplitude is T_{cmax} .

Moreover, the maximum oscillating stress amplitude occurring in the nodal plane at the middle of the transducer is given by:

$$T_{cmax} = Y\mu_0k \tag{12}$$

4.1 Acousto-mechanical analysis of piezoelectric in dynamic condition without pre-load

For a $\lambda/2$ length piezoelectric, when preload is zero ($T_{oc}=0$) and it is excited with a zero-biased alternating voltage, T_{cmax} is limited to the allowable fatigue strength of piezoelectric (see Fig. 2(a)). Using Eq. 8 and considering $T_f=20$ Mpa, $Y=50$ GPa and $c=4,000$ m/s for PZT4 [10] and $\beta=2$ (recommended by author for assuring durable life in high frequency), the maximum allowable power delivered by piezoelectric will be approximately 400 W/cm². From Eq. 12, the displacement amplitude associated with this magnitude of power in 20 kHz is obtained nearly 6.4 μ m. It should be noted that Eq. 4 cannot be used for determination of the amount of voltage amplitude V_m applied on electrodes, as it is for static state. In the theory of vibration, when the damping ratio is small, the ratio of displacement amplitude in dynamic condition to static state is given by reference [12]:

$$\frac{\mu_0}{\mu} = Q_m \tag{13}$$

where μ is a quarter of the thickness change of PZT piece on which DC voltage V is continuously applied and Q_m is the mechanical quality factor.

In high power applications, piezoelectrics with high Q_m are used. The magnitude of this factor in such piezoelectrics is very high (more than 1,000) according to the data sheet offered by most manufacturers [10, 13]. If $Q_m=1,350$ and $d=320 \times 10^{-12}$ m/V for PZT4, the above-mentioned formulas suggest that maximum allowable stress (according to Fig. 2(a))

can be achieved by applying only $29.6V_{amp}$ ($59.3V_{p-p}$) on a single piece PZT ring without pre-stress (as long as there is no restriction in feeding such an amount of power from the power supply). This fact can best describe the risk of using non-prestressed piezoelectric. When n pieces of piezoelectric are employed rather than a single piece and they are connected electrically parallel and mechanically serial, the allowable output power delivered by every PZT ring must be decreased provided that the overall length of all PZT rings together remains $\lambda/2$. As the maximum allowable stress remains the same, the activation voltage for electrically parallel piezoelectric rings must be decreased, i.e. the electric field intensity for a $\lambda/2$ single piece piezoelectric is; $\frac{V_{amp}}{\lambda/2}$ and in multiple-piece transducer with electrically parallel activated piezoelectric rings is; $\frac{V_{amp}}{\lambda/2n} = \frac{nV_{amp}}{\lambda/2}$. Regarding relations 4, 12 and 13, the new value for μ_0 and T_{cmax} will be:

$$\mu_{0n} = \mu_n Q_m = \frac{ndV_{amp}}{2} Q_m = n\mu Q_m = n\mu_0$$

$$T_{cmaxn} = nT_{cmax}$$

Therefore, the activating voltage must be reduced to $\frac{V_{amp}}{n}$ in order to keep the same maximum stress as single piece transducer. This gives the same total power intensity and the power intensity per piezoelectric ring will be;

$$\frac{I}{n} = \frac{400}{n} \text{ W/cm}^2.$$

To increase the power output of the transducer, it is necessary to increase the vibrating amplitude of the transducer ends. As this increase directly increases the nodal stress by the same factor, it is mandatory to have a compressive pre-stress on the piezoelectric pieces to keep $(T_{max})_c \leq \frac{T_{fc}}{\beta}$ (Fig. 2(b)).

4.2 Acousto-mechanical analysis of piezoelectric in dynamic condition under pre-load

In this case, the stress is biased by the pre-stress (T_{oc} ; see Fig. 2(b)). This results in very good coupling coefficient and less mechanical loss in various interfaces and therefore higher efficiency. Since the tensile and compressive fatigue strengths T_f of most piezoelectric ceramics are +25 and -125 MPa, respectively [14], The best pre-stress value seems to be -50 MPa, though consideration for safe operation of the central bolt and mechanical stress depolarization of piezoelectric rings should be made. These restrictions force selection down to $T_{oc}=25$ MPa with $\beta=2$, the allowable cautious stress amplitude is now 37.5 MPa which leads to $\mu_o=24$ μm at 20 kHz, $I=5,625$ W/cm^2 and $V_{\text{amp}}=110.6$ V. In practice, however, higher voltages are required for such power intensity. Meanwhile, the maximum output power intensity that can be tolerated by each PZT ring is much lower than the above-mentioned value. The problem here has arisen from the overestimation of Q_m (=1,350 in this example). The magnitude of this factor varies a lot in different references.¹ For accurate determination of the power of piezoelectrics, the best is to measure oscillation amplitude of manufactured transducer and then calculate the quality factor. The main source of such overestimation is believed to be ignoring the physical effects of prestress, structural (hysteretic) damping through the transducer and the viscous or hysteretic losses of the media in contact with the transducer. In fact, far before mechanical failure, electrical and thermal depolarization restricts the allowable voltage on piezoelectric ceramics.

5 Material selection for backing and matching

Although the most efficient transmission of acoustic energy happens when the two contacting media have the same acoustic impedance [16], it is not easy to find a material whose impedance is equal to piezoelectric's. To have a good material selection for matching and backing the following steps are proposed [10, 16]:

To achieve full percent transmission of ultrasound between PZT ceramics with specific acoustic impedance of Z_c and metal end pieces, the following equation must be satisfied:

$$Z_c = \sqrt{Z_m Z_b} \tag{14}$$

¹ For example, ref. [15] suggests the values of $Q_m=7.5$ and $Q_m=27,500$ for Quartz when oscillating in water and air, respectively.

Where Z_m and Z_b are specific acoustic impedance of matching and backing, respectively. On the other hand, the acoustic impedance ratio of

$$q_i = \frac{Z_c A_c}{Z_i A_i} \tag{15}$$

and ultrasonic power intensity gain coefficient

$$G_i = q_i^2 - (q_i^2 - 1) \sin^2 \frac{\omega_s l_c}{c_c} \tag{16}$$

must be calculated. i denotes to matching or backing metallic end pieces, ω_s is angular resonant frequency, l_c is the partial length of piezoelectric stack located between backing (or matching) and the nodal plane and c_c is sound speed in piezoceramics. The average power intensity radiated to water (having Z_w specific acoustic impedance) by each end piece is given by equation:

$$I_{i \text{ av}} = G_i \left(\frac{T_{c \text{ max}}}{Z_c} \right)^2 (Z_w)/2 \text{ (W/m}^2\text{)} \tag{17}$$

By appropriate selection of material for matching and backing, it is possible to obtain high average-power-intensity radiation in one end and very low average-power-intensity radiation on the other end. Decrease of Z_{ii} and l_c gives higher gain factor.

It is sometimes advisable to make pores and small holes inside the matching layer in order to reduce its acoustic impedance to a further extent. The diameter of pores should be, at least, of two orders less than the wavelength to prevent deterioration of coupling properties. In addition, along with the impedance matching condition, some more and important factors should be considered in material selection including heat conduction, machinability, corrosion tendency as well as mechanical strength of material. Matching and backing layers are recommended to be made of light and heavy materials, respectively, to magnify oscillation amplitude in matching and reduce it in backing [17]. The output vibration amplitude in an ultrasonic transducer used for wire welding increased by 55 and 90% only by replacing stainless steel in matching with Titanium and Aluminum, respectively[18].

In conclusion, the configuration of Aluminum–PZT–Steel is advisable whilst the combination of Magnesium–PZT–Steel is the most qualified configuration for the transducer but it is expensive.

6 Matching, backing and piezoelectric lengths

The most fundamental rule in determination of various axial dimensions in the transducer is that to permit it to operate in resonance, the overall length should be exactly $\lambda/2$

(or a whole coefficient of $\lambda/2$). Since the transducer is not a single body and consists of several parts with different materials and cross-sections along the transducer, the following analytical relationship for one-dimensional longitudinal sinusoidal plane wave propagation in medium is applied [19]:

$$\frac{d^2\mu}{dx^2} + \frac{1}{A} \frac{dA}{dx} \frac{d\mu}{dx} + \frac{\omega^2}{c^2} \mu = 0 \tag{18}$$

The boundary conditions between the parts are: equilibrium of displacement (continuity condition) and force (Newton’s third law) of the two contacting media at the shared plane. Depending on the application and designer’s concerns, other considerations can be made to determine all axial dimensions of the transducer.

Supposing different materials are used as backing and matching, and assuming the nodal plane is located somewhere between the ceramics, the term q_i can be defined as:

$$q_i = \frac{\rho_c c_c A_c}{\rho_i c_i A_i}$$

In practice, A_i is always greater than A_c . Solving equation (18) leads to the following relation applied for each $\lambda/4$ -lengthen part of the transducer in resonance:

$$\text{tg}\left(\frac{\omega_s l_i}{c_i}\right) \text{tg}\left(\frac{\omega_s l_c}{c_c}\right) = q_i \tag{19}$$

where l_i and c_i are, respectively, the length and sound speed of backing (or matching). If the diameter of each part (D) along the transducer divided by the respective quarter of wavelength ($\frac{D}{\lambda/4}$) is significantly greater than unity, the effective sound speed of the first mode considerably falls below $c = \sqrt{Y/\rho}$ (which pertains to one-dimensional wave transmission) and should be modified according to the references [20].

The nodal plane should be in the flange-shaped part of the transducer from where the apparatus is gripped and clamped. Based on the number and the thickness of the PZT rings applied, the flange can be designed in different locations. In the case that too thick ceramics have been used, the nodal plane is preferred to be embedded somewhere between the ceramics. Most designers, however, tend to place this plane just beyond the PZT stack where it reaches the matching mass.

As a good estimation in the process of designing, different axial dimensions of the transducer (Fig. 1)

are approximated to meet the following relationships [21]:

$$\begin{aligned} & \frac{1}{3} \left(\frac{c_m}{2f_{res}} + \frac{c_c}{2f_{res}} + \frac{c_b}{2f_{res}} \right) \langle L_{tot} \langle \min \left\{ \frac{c_m}{2f_{res}}, \frac{c_b}{2f_{res}} \right\} \rangle \\ H_B &= H_{B1} + H_{B2} \geq 0.5H_C, H_C = N_c t_c + (N_c + 1) \cdot t_f \\ 2t_c &\leq H_{B1}, 2t_c \leq H_{F1}, L_{BL} + L_{BF} = L_{Bt} \left(\cong \lambda_B/4 \right) \end{aligned} \tag{20}$$

t_c is the thickness of each piezoceramics, N_c is the number of piezoelectric rings, t_f is the thickness of electrodes, λ_B is the sound wavelength in the bolt and subscripts b and m denote to backing and matching, respectively. Other references [22] suggest the following rules in respect of backing and matching’s thicknesses.

$$H_B > \frac{1}{5} D_B, H_{F1} > \frac{1}{5} D_{F1}, H_{F2} > \frac{1}{5} D_{F2} \tag{21}$$

For assuring that the pre-stress is applied uniformly on the entire surfaces of the piezoceramics, H_{B1} must exceed a minimum. Charles Mischke has proposed an empirically developed approach to determine the area in which stress applied by bolt–nut fastener is almost uniform. Based on his findings, this area is limited to the lines drawn at 45° from the corners of the head (Fig. 4) [23].

For electrical safety and for design restrictions, the number of piezoceramics must be even. For having a high power intensity gain factor (G_I) for matching and a very low value for backing, it is necessary to have low $\frac{l_c}{\lambda_c/4}$ and the wavelength in the ceramic materials is greater than 20 to 30 times the thickness of the ceramics disk or ring. To fulfill this requirement and in the meantime to have a high power output (higher number of ceramic pieces), the design frequency of the ultrasonic head has to be selected as low as possible to permit increase of l_c . On the other hand, decrease of $\frac{l_c}{\lambda_c/4}$ deteriorates the piezoelectric effective coupling coefficient k_{eff}/k_{33} . It must be included that, at

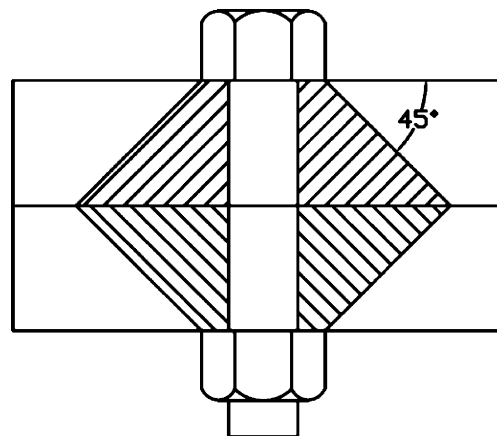


Fig. 4 Charles Mischke’s criterion in uniform stress distribution in a bolted joint

low frequencies, the radiated waves are no longer planar and the right hand side of equation (16) must be multiplied by the real part of radiation coefficient [10]. This real value of coefficient is less than one if the diameter of the radiating face of the transducer is less than $2.5 \lambda_w/4$ (λ_w is sound wavelength in water in design frequency). Therefore, an optimization must be performed for selection of resonant frequency.

7 Matching and backing diameters

Following considerations should be made when determining the diameter of elements: Whole surfaces of PZT rings must be completely covered by the backing and matching masses. Meanwhile, the matching and backing diameters must be equal to or less than twice as much as the piezoelectric rings diameters. In addition, the minimum possible diameter must be designated in order to avoid disturbing shear and lateral modes of vibration. In other words, $\frac{D_i}{\lambda_i/4} < 2$ should be fulfilled (λ_i is calculated for the respective section of the transducer head). Moreover, to have a good approximation of sound speed by relation $c = \sqrt{Y/\rho}$, it is necessary to have $\frac{D_i}{\lambda_i/4} < 1$. If the selected design frequency is low, the radiating face diameter of the transducer must be at least $2.5 \lambda_w/4$ [10].

8 Central bolt

In sandwich transducers, a central bolt or a number of peripheral bolts are required to mount and apply an amount of pre-load on PZT ceramics. The needed torque for fastening the bolt in the former case is considerably higher than that for the latter one. Use of one big central bolt is usually recommended. The advantage here is that the stress applied is more uniform in this way and the efficiency is slightly higher compared with multi-bolted head. Bolt should be selected for enduring life under fatigue loading by considering both static pre-load and acoustical dynamic stress. Since the static friction coefficient is converted to

dynamic one (which is significantly less), one important point here is that the bolt should be fine-threaded. Then the bolt is less likely to loose under operation.

For best acoustic matching with the transducer, the length of the bolt is suggested to be nearly $\lambda/4$ [16]. The empirical data shown in Table 1 can be helpful for assuring a designer upon his/her theoretical calculation. The bolts recommended in this table should have the specifications of DIN912, class 12.9.

If the internal and external mating threads are made of different materials (which is often the case), the threaded length of the bolt (inch) to be screwed into the matching can be given by [24]:

$$L_{BL} = \frac{T_{ut}(\text{external thread})}{T_{ut}(\text{internal thread})} \times \frac{2A_t}{\pi k_n [0.5 + 0.57735 n(E_s - k_n)]} \tag{22}$$

where T_{ut} is the ultimate tensile strength, A_t is tensile–stress area of screw thread (in.²), k_n is minor diameter of internal thread (in.), E_s is pitch diameter of the external thread (in.) and n is the number of threads per inch.

9 Other considerations

The electrodes are of copper–beryllium alloy of 200–250 μm thickness with very high fatigue strength. The soldering tags must be damped with a pliable substance like silicon rubber for preventing breakage due to fatigue. To overcome the reactive current created by the capacity of the piezoelectric ceramics, compensation must be made by inductance L_{par} connected parallel to the piezoelectrics. Its value is given by:

$$L_{par} = \frac{1}{4\pi^2 f_s^2 C_0} \tag{23}$$

Where f_s are series resonant frequency and C_0 is the piezoelectric capacity [10].

Table 1 Approximate empirical recommendations for selection of the central bolt [21].

Power and frequency range	L_{BF} (mm) min/max	L_{BL} (mm) min/max	L_{Bt} (mm) min/max	Approximate bolt size M (mm)	Torque required (N m)
20 kHz 1 kW	40/60	20/30	60/75	10	88/108
20 kHz 2 kW	40/60	25/35	67/78	11	108/127
20 kHz 3 kW	40/60	30/40	75/80	12	127/147
25 kHz 1 kW	30/50	20/30	50/60	10	88/108
25 kHz 2 kW	30/50	25/35	55/65	11	108/127
25 kHz 3 kW	30/50	30/40	60/70	12	127/147

10 Designing the transducer

Based on what already discussed, a typical ultrasonic transducer with the specifications of 3 kW input electrical power, 0~1,000 V AC and 22 kHz frequency is designed, manufactured and tested. For such transducer, the input voltage variation, typical stress variation at nodal plane of piezoelectric and bolt, and piezoelectric and bolt axial deformations have been given in Fig. 2(b) and (c).

10.1 Selection of appropriate Piezoceramics

The intended output acoustical power is the key factor for selection of the number of PZT rings required. The maximum allowable power delivered by each piece of PZT ring not only depends on the quality of piezoelectric material and treatment made during its production processes, but also is highly affected by its dimensions. This power is commonly said to range from 15 to 30 W/cm² [21]. PZT rings are available in standard sizes in market and can very scarcely be found in diameters above 50 mm. This size is chosen in this high power intensity transducer to permit obtaining the highest possible power by one single PZT ring. On the other hand, PZT rings with bigger diameters may cause disturbance by producing lateral shear wave modes. Other dimensions such as thickness and inner diameter are very limited for such a big PZT ring and are selected as 6 and 20 mm, respectively, in this practice.

The piezoelectric rings used are known as HYP42 (equivalent to very well known PZT4) supplied from MPI in Switzerland. Other specifications of these PZT rings are listed in Table 2.

This type of piezoelectric ceramic has low mechanical and dielectric losses. Having a high mechanical quality factor, it can be used in high power applications where oscillation in large displacement amplitude is desired [10]. By considering the transmission surface area of the selected PZTs and taking the output power intensity capability of each PZT ring about 30 W/cm², one single PZT ring can deliver an amount of 500 W. Therefore, to reach the predetermined overall power of 3 kW, at least six pieces of such a PZT ring should be used. Applying some more PZT rings to the transducer without increasing the input supplied

power may cause the transducer to vibrate in higher displacement in unloaded circumstances (oscillation in air). Nevertheless, the preloading bolt will be more at risk of failure, the deliverable force of the transducer will substantially fall and the functional efficiency of the transducer will become highly sensitive to the loading condition [14].

10.2 Stress analysis along the transducer

With a positive DC biased alternative voltage application across the PZT rings, dynamic tensile stress resulted from acoustic wave propagation is added to the compressive pre-stress which statically exists along the whole transducer. The magnitude of this alternating stress is dependent upon the applied voltage, piezoelectric charge constant, resonance frequency, elasticity and sound speed of piezoceramics and above all, mechanical quality factor. Equations 4, 12 and 13 give:

$$T_{c \max} = nY \frac{\omega}{2c} Q_m d_{33} V_{\max} \quad (24)$$

Where $T_{c \max}$ is the maximum alternating stress amplitude, V_{\max} is half the peak-to-peak voltage applied on piezoelectric and n is the number of PZT rings employed. Although Eq. 24 is based on some simplifying assumptions, yet it is quite applicable in mechanical design of the transducer. The best and most reliable way to predict the exact amount of acoustic stress, however, is utilizing FEM and associated software like ANSYS.

The real magnitude of Q_m to be applied in Eq. 24 should be calculated by testing the transducer, measuring the displacement amplitude and substituting into Eq. 13. For simplification of the design process, the empirical data obtained by BRANSON—the pioneer in ultrasonic industry in USA—are used as an approximation. The displacement amplitude at the front head (matching radiating face) of the transducer for 502/932R, 3,000 W, 20 kHz converter which is very similar to the proposed transducer is measured to be around 20 μm [25]. In our study this value is taken as the amplitude of the piezoelectric face. It means that the G_i factor of matching given by Eq. 15 is assumed one. Thus, by Eq. 13 the mechanical quality factor is estimated to be:

$$Q_m = \frac{2\mu_o}{n d_{33} V_{\max}} = \frac{2 \times 20 \times 10^{-6}}{6 \times 320 \times 10^{-12} \times 500} \approx 42 \quad (25)$$

and from Eq. 24:

$$T_{c \max} = 36.7 \text{ MPa} \quad (26)$$

Q_m and $T_{c \max}$ obtained by these calculations are close to reality to a great extent. Consequently, the mechanical damping ratio ($\zeta = \frac{1}{2Q_m}$) [19] in this transducer will be calculated to 0.012 which is acceptable.

Table 2 Specifications of HYP42 by MPI.

Specifications		Value
Dielectric constant	$\epsilon_{33}^T / \epsilon_o$	1,450
Electromechanical coupling factor	K_{33}	0.72
Piezoelectric charge constant	d_{33}	$320 \times 10^{-12} \text{ C/N}$
Piezoelectric voltage constant	g_{33}	$28 \times 10^{-3} \text{ V m/N}$
Elastic compliance	S_{33}^E	$19 \times 10^{-12} \text{ m}^2/\text{N}$
Mechanical quality factor	Q_m	1,350

10.3 Central bolt

Table 1 suggests application of M12 for the transducer with power capacity of 3 kW. This bolt is equivalent to the USA standard bolt UNF20, 1/2". Since the recommendations of this table pertain to fine and well-treated American bolts, while there was not such reliance on the Metric bolts in Iranian Market, M16×1 with the following specifications was chosen:

Hexagon Socket Head Cap Screw, DIN912 M16 × 1
 × 75, 12.9

To be in the safe side, the prestress on the piezoelectric pieces was taken −34 MPa (rather than −50 MPa) to assure enduring life of the bolt under fatigue loading.

10.4 Static stress in the central bolt

In the static state, the tension force in the bolt is equal to the compressing force in the piezoceramics, i.e.:

$$\frac{T_{ob}}{T_{oc}} = \frac{A_c}{A_b} \tag{27}$$

By substituting the cross section of the PZT and the tensile–stress area of the bolt (15.06 mm dia.) into Eq. 27, the tension stress of the bolt corresponding to $T_{oc} = -34$ MPa will be calculated as $T_{ob} = 315$ MPa.

10.5 Dynamic stress and total stress in the central bolt

From Eq. 12, the maximum stress amplitude in the bolt with $Y = 200$ GPa, $\mu_o = 20$ μm and $c = 5,800$ m/s will become 95 MPa (maximum amplitude of vibration of the transducer has been assumed to be as the amplitude of the end face of the piezoelectrics). Therefore, the total stress will be $315 + 2 \times 95 = 505$ MPa. For the selected bolt (DIN912M16×1, Class12.9), ultimate tensile strength (T_{ut}) is about 1,200 MPa, axial endurance limit for bolt (S'_e) is half of that (600 MPa) and fatigue strength reduction factor (K_f) is reported to be 3 for rolled bolt. This results in 200 MPa endurance fatigue strength. Using the Goodman criterion, the safety factor of 1.33 is resulted [23].

10.6 Determining the length of the bolt

According to Charles Mischke criterion (Fig. 4), for the diameter of $\phi 24$ mm for the bolt head and $\phi 50$ mm outer diameter of the PZT, the minimum H_{B1} (Fig. 1) is 13 mm which is greater than twice as the PZT thickness. As there are 6 pieces of PZT rings with the thickness of 6 mm and seven pieces of electrodes with the thickness of 0.25 mm, the total length, H_C , will reach 37.75 mm. In addition, from Eq. 22 ($n = 25.4$, $A_t = 0.276$ in.², $k_n = 0.882$ in. and $E_s = 0.604$ in.), and by using the specifications given in Table 3, the minimum thread length of the bolt to be screwed into the matching should be 18 mm. Failure of the matching is more costly than that of the bolt. Therefore, it is wise to screw more threads of the bolt into the matching to assure protection of the matching threads against shear stress. The safety factor of 1.4 will result in the total L_{BL} of 25 mm and thus, the nominal length of the bolt L_{BT} is about 75 mm. As a result, the bolt will be chosen with the specifications as already described.

10.7 Materials of backing and matching

On the basis of what already discussed, the most common configuration of Steel–PZT–Aluminum was used in the construction of the transducer. Selection of an appropriate standard code for steel and aluminum is of great significance. St303 or St304 for backing and Al7075-T6 for matching are suggested as suitable materials due to their good acoustic properties and acceptable performance in practice [25, 26]. These materials were provided in the present study. The necessary specifications of all the components of the transducer are listed in Table 3.

10.8 Measurement of acoustic impedance of materials

As the exact value for density and sound velocity of materials will be utilized in the design process, these two properties were accurately measured for backing, matching and Piezoceramics used.

Measuring the sound velocity This measurement was made in the NDT Laboratory by using ultrasonic equipment

Table 3 Material specifications of the transducer's components.

Part name	Material	Standard code	Sound velocity (m/s)	Density (kg/m ³)	T_{ut} (MPa)	T_{yt} (MPa)
Backing	Stainless steel	St304	5,720	7,868	–	–
Matching	Aluminum	Al 7075-T6	6,210	2,823	618	–
Central bolt	Alloy steel	DIN912, M16×1, Class 12.9	5,800	–	1,210	1,000
Electrode	Nickel 99%	–	4,970	8,908	–	–

ASCANWIN, E2.58, 2002. The time of flight (TOF) of the pulse which was transmitted and received by a single probe of 2 MHz, $\Phi 24$ was measured (Fig. 5). By knowing the thickness of the specimens, the following sound velocities were obtained by a simple calculation: The maximum deviation of the measured data from the above mentioned results were roughly ± 10 m/s.

Measuring the density A very accurate mechanical balance KERN 2000, 0.0001 g resolution, made in Switzerland was employed. The mass of materials was readily measured by this balance. For measuring the volume, however, Archimedes’ law was applied. According to this law, if m is the measured mass in air and m' is the measurement of the same mass but suspended in pure water ($\rho = 1 \text{ g/cm}^3$) medium, the volume of the mass is derived by:

$$V = m - m' \tag{28}$$

Using Eq. 28 as well as $\rho = m/V$, the density of all three specimens was obtained as:

$$\rho_{st} = 7868 \quad \rho_{piezo} = 7640 \quad \rho_{Al} = 2823 \text{ kg/m}^3$$

Maximum deviation of measurements made in several trails was $\pm 2 \text{ kg/m}^3$.

10.9 Determination of diameters

By observing all the considerations already explained, following diameters were determined (Fig. 1):

$$D_B = 51 \text{ mm} < \lambda_{steel}/4 = 65 \text{ mm},$$

$$D_{F1} = 64 \text{ mm} < \lambda_{Al}/4 = 71 \text{ mm}$$

$$2.5\lambda_{water}/4 = 40 \leq D_{F2} = 40 \text{ mm} < \lambda_{Al}/4 = 71 \text{ mm},$$

$(c_{water} = 1400 \text{ m/s})$

The inner diameters should be designed with consideration of embedding a central bolt of $M1$ through backing and matching with the least possible clearance.

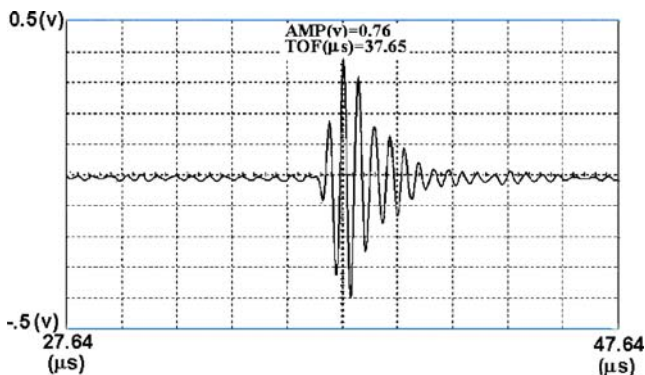


Fig. 5 Measuring sound velocity using ultrasonic NDT equipment

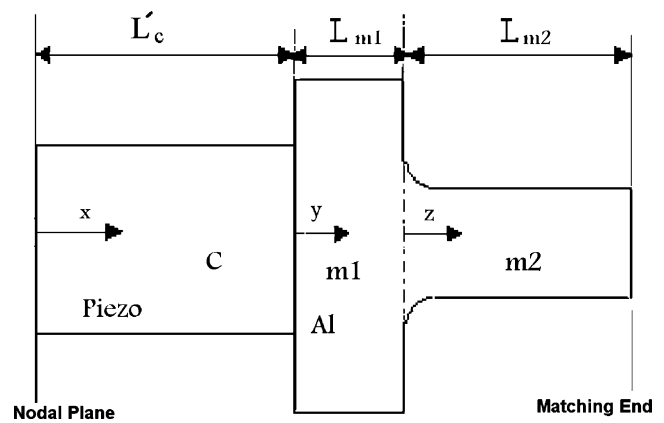


Fig. 6 Half of the transducer, from the nodal plane to the end of the matching mass

10.10 Locating the nodal plane

The closer the nodal plane is to the matching layer, the shorter the backing block will be. The best place for the node is the flange-shaped part of the matching, not only because of the feasibility of fixing the transducer body but also because aluminum has more strength than PZT against dynamic stress, which is maximum at the nodal plane. Nonetheless, the selected PZT rings in this practice are so thick that the length of backing will become unacceptably small (6.5 mm). Therefore, clamping feature will be designed to be on horn or booster attached to the matching of the transducer. Yet, the nodal plane should be as close to the matching as possible. The explanation is that, the more the length of matching is, the more stable condition the transducer will function under [14]. The minimum possible length for backing should be considered correspondingly.

10.11 Determination of Backing Length:

Noting the previously designed $H_{B1} = 13$ mm and bolt head size (16 mm), the overall length of backing is designed 29.5 mm to permit the bolt head to be embedded in backing.

10.12 Determination of Matching Length

First, the exact location of nodal plane should be determined. Applying Eq. 19 for the first $\lambda/4$ of transducer including backing leads to $L_c = 21.55$ mm. This means that the nodal plane is almost at the middle of PZT stack. Figure 6 illustrates the other half of the transducer, from the nodal plane to the end of the matching mass. Eq. 18 is simplified to the following differential equation

for each section through which the cross-section is constant:

$$\frac{d^2 \mu}{dx^2} + k^2 \mu = 0 \tag{29}$$

$$\mu_i = C_1 \cdot \sin k_i x + C_2 \cdot \cos k_i \cdot x$$

$$T_i = Y_i \frac{d\mu_i}{dx} = Y_i \cdot C_1 \cdot k_i \cdot \cos k_i x - Y_i \cdot C_2 \cdot k_i \cdot \sin k_i x \tag{30}$$

From the assumptions already made, $Y = c^2 \rho$ is applied in the above equation for simplification. Applying the following boundary conditions:

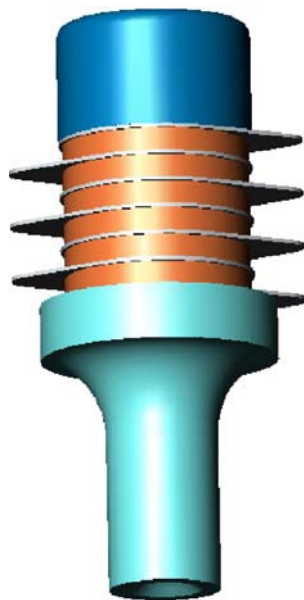
$$\begin{aligned} \mu_c(x = 0) &= 0 \\ \mu_c(x = L'_c) &= \mu_{m1}(y = 0), T_c(x = L'_c) \cdot A_c = T_{m1}(y = 0) \cdot A_{m1} \\ \mu_{m1}(y = L_{m1}) &= \mu_{m2}(z = 0), T_{m1}(y = L_{m1}) \cdot A_{m1} = T_{m2}(z = 0) \cdot A_{m2}, \\ \frac{d\mu_{m2}}{dx}(z = L_{m2}) &= 0 \end{aligned}$$

and solving the equation separately for each section of c , m_1 and m_2 and supposing $L_{m1} = 10$ mm, L_{m2} will be; $L_{m2} = 57.5$ mm and consequently the total length of the transducer will become: $L_{tot} = 134.7$ mm.

10.13 Isolating bush

To avoid short-circuit by probable contact between central bolt and the electrodes and to keep backing and matching connected to ground, it is necessary to make use of isolating bushes placed around the bolt shank. Such bushes can be made of PVC or Polyamides. The designed transducer is shown in Fig. 7.

Fig. 7 Final designed transducer



11 Assembling the transducer

There are two techniques available to make sure that the desired amount of pre-stress is already applied on PZT rings while fastening the central bolt:

1. Using Torque Meter

The relationship between the tension force made in bolt and the torque applied on it for fastening is:

$$T = KdF \tag{31}$$

where K is a constant factor proposed in references for different friction conditions and is found to be 0.189 in this case [23], d is the nominal bolt diameter and F is the tension force in bolt. For having the pre-stress of 34 MPa on PZT rings, the corresponding tension force in the central bolt shall be around 56 kN and consequently, the required torque to apply such compression on PZT rings will be calculated about 169 Nm. Moreover, this amount is advised to increase by approximately 10% to 186 Nm to compensate the looseness of the bolt after assembling [14].

2. Measuring the charge generated on PZT rings

Use of torque meter for measuring the bolt torque is not a reliable method. A better solution is the use of volt-meter and measurement of the produced charge on electrodes resulted from the pre-stress. By using the constitutive equations in piezoelectrics, the overall charge generated on n pieces of PZT rings with area of A and under static stress of T_{oc} will be given by [11]:

$$Q_{tot} = n d_{33} A T_{oc} \tag{32}$$

This equation suggests that in this case of study, the total amount of charge is 108 μ C.

There are three considerations, which make it essential to parallel a few μ F capacitor with PZTs while fastening the central bolt and measuring the voltage generated by the charge: first, without adding such a capacitor, the produced voltage on the electrodes will reach up to 5,114 V which is hazardous. Secondly, due to the high amount of voltage generated, the piezoelectric rings show a very high stiffness. Therefore, the PZT stack will considerably loose after being discharged and consequently they lose the required pre-stress. Finally, the generated charge is so small and the open-circuit voltage is so high which makes voltage measurement impossible as the small capacity piezoelectrics are discharged through the voltmeter resistance. Thus, the best solution is to reduce the open-circuit voltage to one volt by a parallel capacitor to provide enough time for accurate voltage measurement during fastening time. The capacitance of the piezoelectric is often much less than that of the paralleled capacitor (21,165 pF compared with App.

100 μF). Therefore, the overall capacitance of the transducer along with the added capacitor C_s will then be:

$$C_{\text{tot}} = 6 \times C_c + C_s \approx C_s \quad (33)$$

and the corresponding voltage on each piezoelectric is:

$$U = \frac{Q_{\text{tot}}}{C_{\text{tot}}} = \frac{nd_{33}AT_{\text{oc}}}{C_s} \quad (34)$$

The use of a capacitor with $C_s=10 \mu\text{F}$ is of common interest [10]. Nonetheless, to lengthen the time required for fastening and to reduce the undesirable discharge, which occurs in measurement process of the produced voltage using a voltmeter, a 125 μF capacitor was chosen. This leads to the generation of 0.864 V resulted from 34 MPa pre-stress on piezoceramics. With considering 10% looseness of the bolt after assembly, the central bolt was fastened to such extent that the produced voltage on the added capacitor reach 0.95 V (Fig. 8).

12 Test of the transducer by network analyzer

Impedance matching of the electromechanical transducer with the electric power driver is the key factor in operation of the piezoelectric transducer. Using Network Analyzer is the best method of measuring the specification of the transducer such as the equivalent resistance (R), capacitance (C) and inductance (L) as well as series and parallel resonance frequencies. The test was done by Rohde and Schwarz, sweeping frequency within 9 kHz–4 GHz, resolution of 10 Hz. The sweeping frequency was set between 10 kHz to 30 kHz and phase-versus-frequency diagram was drawn (Fig. 9) in which series and parallel frequencies are both illustrated. The measurement was made with the transducer loaded and unloaded. It should be noted, however, that simulation of the loading condition

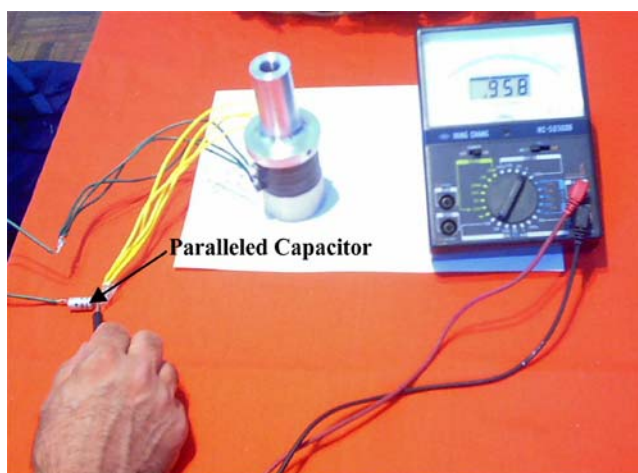


Fig. 8 Measuring the charged voltage on the added 125 μF capacitor just after fastening the bolt

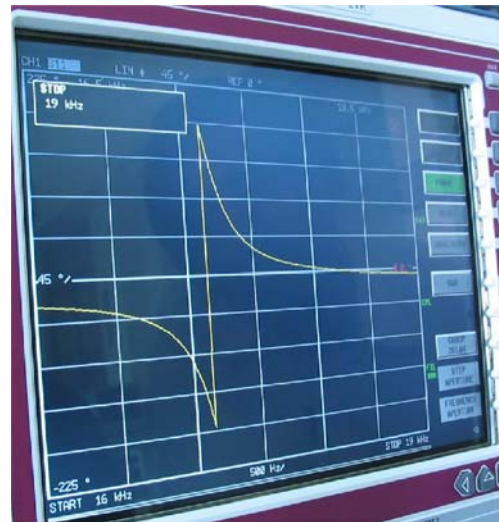


Fig. 9 Diagram of phase versus frequency in the developed transducer in unloaded condition

is greatly dependent upon the transducer application. In this practice, the simulation was carried out by manually pushing the transducer against a wooden desk. The back force was approximately 20 kg F by hand (Fig. 10).

The results show that the series and parallel frequencies are $f_s=17,200 \text{ Hz}$ and $f_p=17,250 \text{ Hz}$, respectively. It can be inferred from this slight difference that the transducer has been made so finely and neatly that the Q_m is relatively high [26]. Moreover, variation of the load on the transducer shifted the resonance figure very marginally (less than 200 Hz). As a result, the Self-Tuning system in power supply should be able to change the frequency within 400 Hz (after considering a safety factor of 2).

There was a considerable difference between the real resonance frequency and the intended one in designing process. This error results from the simplifications made in analyzing the wave propagation through the transducer.



Fig. 10 Measuring the impedance characteristics of the developed transducer using Network Analyzer

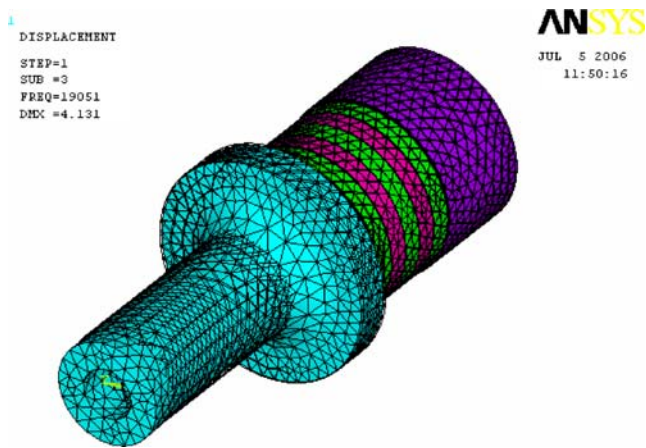


Fig. 11 Full 3D modeling with SOLID227 elements used for piezoelectric and SOLID98 elements used for other components

One of the most troublesome simplifications is assumption of one-dimensional wave transmission and the use of $c = \sqrt{Y/\rho}$. If lateral strains are also taken into account by applying the general relationship of Yung’s module substituted into Eq. 18, the designed length of the transducer will be lower and this leads to decline of the error in frequency by half [11]. In addition, interior mechanical damping of the transducer is omitted when considering the length of $\lambda/2$ as the optimum resonant length, while structural (hysteretic) damping of energy are always present in material which shifts the resonant frequency down.

13 FEM modeling of the transducer (modal analysis)

Natural frequency and mode shape are very important parameters in the design of an ultrasonic transducer for dynamic loading conditions. To verify the characteristics of the transducer, FEM modeling was used by employing ANSYS software. In ANSYS analysis, the transducer

geometry was treated as a 2D axisymmetric model using the PLANE13 and PLANE223 element types and 3D quart and full 3D model using SOLID5, SOLID98 and SOLID227 element types (see Fig. 11). The modeled transducer was used in modal analysis to understand its mechanical behavior and to inspect its natural frequency and to find location of the node. The axial relative motion of the matching tip was of particular interest in this study. The structural damping was ignored, although, the amplitude on the tip of the matching must definitely be influenced by damping. It must also be noted that this model ignores presence of the electrically insulating mechanically aligning polymer bushes, normally used inside the piezoelectric ring’s hole around the clamping bolt shank. These bushes are not stressed in preloading of the piezo-ceramic stack during the assembly. The results showed a good agreement between the network analyzer and the modal analysis frequencies (see Table 4).

14 Conclusion

In this study, the general principles of designing ultrasonic transducers using piezoelectrics for high power applications were discussed and a typical transducer of 3 kW was developed and tested by Network Analyzer. The analysis done shows that the nominal power capacity of piezoelectric rings is affected by the pre-stress applied and the optimum such pre-stress is between 25 and 50 MPa for assuring the safe and enduring life of piezoceramics under high-intensity loads. It was argued that using sandwich structure in piezoelectric devices increase the allowable output power delivered by every PZT ring. Although the more pieces of piezoelectric are employed, the greater the displacement amplitude will be in unloaded condition, unnecessarily increasing the number of PZTs used in the transducer is not advised since it makes the transducer very sensitive to the application and loading condition. The constitutive

Table 4 Resonance and anti-resonance frequencies for the FEM modeling of the transducer.

Modeling type	Polarized axis	Element type of piezo.	Element type of other components	Element size (mm)	Nominal resonance Freq. (kHz)	Resonance freq. (kHz) from FEM-modal	Anti-resonance (kHz) from FEM-modal	Measured resonance freq. by network analyzer (kHz)	Time spent for modal analysis (min)
2D	Y	PLANE 13	PLANE 13	1	22	17.308	18.969	17.2	<1
2D	Y	PLANE 223	PLANE 13	1	22	17.308	18.969	17.2	<1
1/4 3D	Z	SOLID5	SOLID5	1	22	17.309	18.970	17.2	20
1/4 3D	Y	SOLID227	SOLID98	4	22	17.329	18.984	17.2	1
Full 3D	Y	SOLID5	SOLID5	4	22	17.418	19.142	17.2	1
Full 3D	Y	SOLID5	SOLID5	2.5	22	17.368	19.055	17.2	1
Full 3D	Y	SOLID227	SOLID98	2.5	22	17.311	18.970	17.2	60

piezoelectric equations mentioned in most sources and books are not valid for analyzing the acoustical dynamic stress in ultrasonic transducers. Instead, the analysis should be done with considering the dynamic behavior (elastic, damping and Inertia factors) of the problem. In dynamic analysis of the transducer, if internal losses (structural hysteretic damping) are ignored, a noticeable error will occur particularly in determining the resonant frequency. Furthermore, simplifying presumption of one-dimensional wave propagation along the transducer will lead to error in design of the transducer; especially for high power ones which have bigger cross sections. Comparison of the modal analysis results obtained from different 2D axisymmetric and 3D modeling techniques proved that there is a good agreement between the results achieved from the network analyzer and the FEM modeling.

Acknowledgements This work was funded by Highly-Distinguished Solid Mechanics Center at AmirKabir University of Technology. Thanks should also be given to Advanced Manufacturing Research Center (AMRC) for their contribution to manufacture the parts, and to Electromagnets Laboratory of Electrical Department of AmirKabir University of Technology where the required equipments were provided to test the transducer. Authors express their sincere appreciation to Dr. Prokic and his colleagues at MPInterconsulting for providing invaluable empirical data and helpful comments.

References

1. W.P. Mason, *Electromechanical Transducers and Wave Filters* (Van Nostrand, Princeton, NJ, 1948)
2. W.P., Mason, *Piezoelectric Crystals and their Applications to Ultrasonic* (Van Nostrand-Reinhold, Princeton, NJ, 1950)
3. H. Allik, T.J.R. Hugues, *Int. J. Numer. Methods Eng.* **2**, 151–157 (1970)
4. D. Boucher, M. Lagier, C. Maerfeld, *IEEE Trans. Sonics Ultrasonic.* **28**, 318–330 (1981)
5. E. Mori, et al, *Ultrasonic International 1977 Conference Proceeding*, p. 262, 1977
6. E. Mori, Y. Tsuda, *Proceeding of Ultrasonic International*, pp. 307–312, 1981
7. L. Shuya, *Appl. Acoust.* **44**, 249–257 (1955)
8. S. Hirase et al., *Ultrasonics*, **34**, 213–217 (1996)
9. D.J. Powell, G. Hayward, R.Y. Ting, *IEEE Trans. Ultrason Ferroelect. Freq. Contr.* **45**(3), 667–679 (1998)
10. J. Randraat, *Piezoelectric Ceramics* (Mullard, London, 1974), p. 5
11. M. Shahini, A. Abdullah, M. Rezaei, *Design and Manufacture of an Ultrasonic Transducer with 1 kW Power and 22 kHz Frequency Using Piezoceramics*. Master of science thesis, Faculty of Mechanical Engineering, AmirKabir University of Technology, 2004
12. F.S. Tse, I.E. Morse, R.T. Hinkle, *Mechanical Vibrations, Theory and Applications*, 2nd edn. (Allyn and Bacon, Boston, MA, 1978)
13. Data Book, *Piezoelectric Crystals* (Finnsonic, Finland, 1997)
14. M. Prokic, *Piezoelectric Transducers Modeling and Characterization* (MPInterconsulting, Switzerland, 2004)
15. W. Seto, *Theory and Problems of Acoustics* ((McGraw-Hill, New York, 1971), p. 188
16. R. Frederick, *Ultrasonic Engineering* (Wiley, New York, 1965), p. 284
17. M. Toda, *Ultrasonic Transducer Having Impedance Matching Layer*. US Patent no. 0027400, 2002
18. H. Leung, M. Wai, L. Wa Chan, C. Kee Liu, *Ultrasonic Transducer*. US Patent no. 0062395 A1, 2003
19. A. Abdullah, *Electro-Physical Processes, Postgraduate Lecture Notes*. Faculty of Engineering, Tarbiat Modarres University, 1991
20. Morgan Electro Ceramics Web Site, *Piezoelectric Ceramics Properties and Applications*, Chapter 6
21. M. Prokic, *BLT Common Recommendation Regarding Dimensions* (MPInterconsulting, Switzerland, 2004)
22. H.A. Rijna, *Proceedings of NATO Advanced Study Institute*, 225–249 (1980)
23. J.E. Shigley, *Mechanical Engineering Design* ((McGraw-Hill, New York, 1986), pp. 305–306
24. E. Oberg, F.D. Jones, *Machinery's Handbook* (Industrial, New York), pp. 1415–1416
25. M. Prokic, *Nodal Plane Position and Output Amplitude* (MPInterconsulting, Switzerland, 2004)
26. A. Shahidi, F. Keymaram, F. Farahmand, *Design and Manufacture of Ultrasonic Cutter for Surgery*. Master of science thesis, Department of Mechanical Engineering, Sharif University of Technology, 2004